AtINO80 represses photomorphogenesis by modulating nucleosome density and H2A.Z incorporation in light-related genes

Chuanwei Yang[a,1], Liufan Yin[b,1], Famin Xie[a], Mengmeng Ma[b], Sha Huang[a], Yue Zeng[a], Wen-Hui Shen[b,c], Aiwu Dong[b], and Lin Li[a,2]

[a]State Key Laboratory of Genetic Engineering and Institute of Plant Biology, Institute of Plant Biology, School of Life Sciences, Fudan University, Shanghai 200438, People's Republic of China; [b]State Key Laboratory of Genetic Engineering, Collaborative Innovation Center of Genetics and Development, International Associated Laboratory of CNRS-Fudan-HUNAU on Plant Epigenome Research, Department of Biochemistry, Institute of Plant Biology, School of Life Sciences, Fudan University, Shanghai 200438, People's Republic of China; and [c]Institut de Biologie Moléculaire des Plantes, CNRS, Université de Strasbourg, 67084 Strasbourg, France

Edited by Christian Fankhauser, University of Lausanne, Lausanne, Switzerland, and accepted by Editorial Board Member Joseph R. Ecker November 11, 2020 (received for review February 4, 2020)

Photomorphogenesis is a critical developmental process bridging light-regulated transcriptional reprogramming with morphological changes in organisms. Strikingly, the chromatin-based transcriptional control of photomorphogenesis remains poorly understood. Here, we show that the *Arabidopsis* (*Arabidopsis thaliana*) ortholog of ATP-dependent chromatin-remodeling factor AtINO80 represses plant photomorphogenesis. Loss of AtINO80 inhibited hypocotyl cell elongation and caused anthocyanin accumulation. Both light-induced genes and dark-induced genes were affected in the *atino80* mutant. Genome-wide occupancy of the H2A.Z histone variant and levels of histone H3 were reduced in *atino80*. In particular, AtINO80 bound the gene body of *ELONGATED HYPOCOTYL 5* (*HY5*), resulting in lower chromatin incorporations of H2A.Z and H3 at *HY5* in *atino80*. Genetic analysis revealed that AtINO80 acts in a phytochrome B- and HY5-dependent manner in the regulation of photomorphogenesis. Together, our study elucidates a mechanism wherein AtINO80 modulates nucleosome density and H2A.Z incorporation and represses the transcription of light-related genes, such as *HY5*, to fine tune plant photomorphogenesis.

AtINO80 | photomorphogenesis | nucleosome | H2A.Z | transcription

Plants continually sense the surrounding environmental conditions to adjust their growth and development. Among them, light is one of the most important external signals affecting plant physiology and developmental processes. Upon exposure to light, etiolated (dark grown) seedlings initiate photomorphogenesis, resulting in a switch to deetiolated morphologies such as cessation of hypocotyl elongation, cotyledon opening, and the accumulation of anthocyanins/chlorophyll (1).

Plants have evolved a series of sensory photoreceptors to perceive and respond to light signals of different wavelengths: red and far-red light-absorbing phytochromes (phyA–phyE), blue/ultraviolet (UV)-A light-absorbing cryptochromes (cry1 and cry2), and UV-B sensing photoreceptor (UVR8) (2). These photoreceptors promote photomorphogenesis by regulating the function of a group of CONSTITUTIVE PHOTOMORPHOGENIC (COP)/DEETIOLATED (DET)/FUSCA (FUS) proteins (3). COP1 is a RING finger E3 ubiquitin ligase that targets a number of photomorphogenesis-related factors, such as ELONGATED HYPOCOTYL5 (HY5), HY5 HOMOLOG (HYH), and PHYTOCHROME RAPIDLY REGULATED1 (PAR1), for proteasome-mediated degradation, resulting in the desensitization of light signaling (4, 5). HY5 is a basic leucine zipper (bZIP) transcription factor required for photomorphogenesis under all wavelengths of light (6). The abundance of HY5 is inversely correlated with the extent of hypocotyl growth (7). HY5 binds to the promoters of over 3,000 genes with diverse functions in plant growth and development (8). Recent studies have suggested that the COP/DET/FUS group of proteins and a group of basic helix loop helix (bHLH) transcription factors PHYTOCHROME-INTERACTING FACTORs (PIFs) act coordinately to repress photomorphogenesis both phenotypically and biochemically (9, 10). PIF proteins (PIF1, PIF3, PIF4, PIF5, PIF7, and PIF8 in *Arabidopsis* [*Arabidopsis thaliana*]) accumulate in the dark and regulate gene expression to promote skotomorphogenesis, or dark-mediated development (11).

In addition to these sequence-specific transcription factors, accumulating evidence indicates that chromatin modifications participate in photomorphogenesis and skotomorphogenesis by acting as transcriptional coregulators. The increased acetylation of histone H3 and H4 in the promoter of the pea (*Pisum sativum*) *PetE* gene is correlated with its light-induced transcription (12). The *Arabidopsis* histone acetyltransferases TBP-ASSOCIATED FACTOR1 (TAF1)/HAF2 and GENERAL CONTROL NONDEREPRESSIBLE 5 (GCN5) are required for the light regulation of growth and gene expression (13). The histone deacetylase HDA15 has been reported to interact with PIF3 to repress the expression of chlorophyll biosynthetic genes (14), while PIF1 regulates the transcriptional network controlling seed germination (15), and HY5 represses hypocotyl cell elongation (16). PICKLE (PKL), an ATP-dependent chromatin remodeling factor, interacts with HY5 to affect H3K27me3 levels in cell elongation genes and negatively controls photomorphogenesis (17). The Switch/Sucrose Non-Fermentable (SWI/SNF) chromatin remodeler subunit BRG1/BRM-associated factor 60 (BAF60) binds

Significance

INO80 is an evolutionarily conserved protein in eukaryotes. Mutations of *INO80* cause growth arrest and embryo mortality in fruit flies and mice, which limits the investigation of INO80 biological functions during morphogenesis of multicellular organisms. Here, we show that AtINO80 interconnects with a light signaling pathway in *Arabidopsis* plants. Our characterization of *atino80* mutants uncovers critical roles of INO80 in nucleosome density and H2A.Z incorporation during plant photomorphogenesis.

Author contributions: W.-H.S., A.D., and L.L. designed research; C.Y., L.Y., F.X., M.M., S.H., and Y.Z. performed research; and L.L. wrote the paper.

The authors declare no competing interest.

This article is a PNAS Direct Submission. C.F. is a guest editor invited by the Editorial Board.

[1]C.Y. and L.Y. contributed equally to this work.

[2]To whom correspondence may be addressed. Email: linli@fudan.edu.cn.

This article contains supporting information online at https://www.pnas.org/lookup/suppl/doi:10.1073/pnas.2001976117/-/DCSupplemental.

First published December 14, 2020.

nucleosome-free regions of multiple G box-containing promoters to oppose PIF4-mediated hypocotyl elongation (18). The H3K36me3 readers MORF-RELATED GENE 1/2 (MRG1/2) interact with PIF7 and recruit histone acetylases to regulate the expression of shade-responsive genes (19). More recently, the photomorphogenesis regulator DET1 has been reported to be essential for the regulation of histone H2B monoubiquitination by controlling the degradation of the SAGA-like deubiquitination module (20). In general, chromatin structure can also be modulated via the replacement of a canonical histone such as H2A with a variant histone such as H2A.Z, leading to gene expression changes (21, 22). Nevertheless, a mechanism by which the incorporation/eviction of histone variants modulates photomorphogenic responses remains mostly unknown.

In this study, we identified the ATP-dependent chromatin remodeling factor INOSITOL REQUIRING80 (INO80) as a key regulator of photomorphogenesis and H2A.Z-mediated gene expression in response to light. The founding member of the Ino80 family is the yeast INO80 protein, which is conserved across eukaryotes (23). A previous study showed that AtINO80 increased local H2A.Z enrichment levels within chromatin regions of the flowering-repressor genes *FLOWERING LOCUS C* (*FLC*) and *MADS AFFECTING FLOWERING* (*MAF*) *4* and *MAF5* (24). While the depletion of *INO80* in yeast does not change the global level of chromatin-bound H2A.Z, it does cause an extensive reorganization of H2A.Z localization across the genome (25). The mutation of *INO80* in *Drosophila melanogaster* and mice (*Mus musculus*) causes growth arrest (26) and early embryo death (27).

Here, we report that *Arabidopsis atino80* mutants exhibit hypersensitivity to light. We investigated the regulation of AtINO80 function at the transcriptional and translational levels and then performed transcriptome deep sequencing (RNA-seq). AtINO80-regulated genes and light-regulated genes showed a significant overlap. We verified by RT-qPCR that AtINO80 regulates the transcription of *HY5* and several light-responsive genes. A reduction of the histone H3 levels and of the H2A.Z enrichment was observed in *atino80* mutants, suggesting a role for AtINO80 related to nucleosome density and H2A.Z incorporation into chromatin. Associated with H2A.Z and H3 reduction, we detected an increased expression for *HY5* as well as other light-responsive genes, in agreement with the light-hypersensitive photomorphogenesis phenotype of the *atino80* mutants. Genetic analysis revealed that *AtINO80* acts in a *phyB*- and *HY5*-dependent manner.

Results

***AtINO80* Is a Repressor of Photomorphogenesis.** A previous study showed that the *atino80-5* and *atino80-6* mutants are *AtINO80* loss-of-function mutant alleles (24). We compared the fluence rate responses of these mutants to those of wild-type Col-0 when grown under red, white, blue, or far-red light (Fig. 1 *A* and *B* and *SI Appendix*, Fig. S1). Increasing light intensity inhibits hypocotyl growth in Col-0. In the dark, the hypocotyls of *atino80* mutants were slightly shorter than those of Col-0 seedlings. However, *atino80* mutants displayed higher sensitivity to all four light conditions tested when hypocotyl length was normalized to dark-grown hypocotyl growth, primarily at lower fluence rates (Fig. 1 *A* and *B* and *SI Appendix*, Fig. S1).

Since hypocotyl growth is mostly driven by cell elongation and proliferation, we measured cell length in the elongation zone of the hypocotyl by microscopy. In agreement with their shorter hypocotyl phenotype, *atino80* mutants showed reduced cell lengths compared to Col-0 under red, blue, and far-red light conditions (Fig. 1*C* and *SI Appendix*, Fig. S2). A slight reduction of cell lengths was also observed in dark-grown *atino80* mutants (*SI Appendix*, Fig. S2*A*). These results indicate that *AtINO80* predominantly regulates cell elongation during hypocotyl growth under different light conditions. Anthocyanin accumulation represents another independent photomorphogenic response, for which we observed elevated anthocyanin contents in *atino80* mutants (Fig. 1*D*).

Taken together, our observations indicate that *AtINO80* acts as a repressor of photomorphogenesis by promoting hypocotyl cell elongation and inhibiting anthocyanin accumulation.

Regulation of *AtINO80* by Light. To determine how light influences *AtINO80* expression, we first measured *AtINO80* mRNA levels when dark-grown Col-0 seedlings were transferred to light. As shown in Fig. 2*A*, *AtINO80* transcript levels decreased slowly by ~50% following 8 h of light exposure. In addition, *AtINO80* transcript levels were up-regulated relative to Col-0 in the *phyB-9*, *phyA-211*, and *cry1* mutants in red, far-red, and blue light, respectively (Fig. 2*B*), suggesting that the light-mediated repression of *AtINO80* expression is facilitated by both phytochrome and cryptochrome photoreceptors.

Next, we assessed AtINO80 protein levels in *35S::AtINO80-Flag* transgenic lines through immunoblot analysis. We observed an increase in AtINO80 protein levels during the transition from darkness into light conditions in independent transgenic lines (Fig. 2*C* and *SI Appendix*, Fig. S3*A*); conversely, AtINO80 protein levels decreased when the transition was oppositely performed from light into darkness (Fig. 2*D* and *SI Appendix*, Fig. S3*B*). We detected more AtINO80 protein in seedlings grown in strong white light (120 μE) than in seedlings grown in the dark or under weak white light (4 μE) (Fig. 2*E* and *SI Appendix*, Fig. S3*C*). The mRNA levels of *AtINO80-Flag* in *35S::AtINO80-Flag* transgenic lines were not regulated by light (*SI Appendix*, Fig. S3*D*). Compared to the control, we documented higher AtINO80-Flag protein levels upon treatment with MG132, a 26S proteasome inhibitor, suggesting that AtINO80 is degraded by the 26S proteasome pathway in the dark (Fig. 2*F* and *SI Appendix*, Fig. S3*E*).

To further investigate AtINO80 protein levels, we generated *pEYFP-AtINO80-G* transgenic seedlings (in which the expression of the *enhanced YELLOW FLUORESCENT PROTEIN* (*EYFP*)-*AtINO80* construct is driven by the At*INO80* native promoter) (24). Consistent with the endogenous *AtINO80* gene regulatory pattern (Fig. 2*A*), the mRNA levels of *EYFP-AtINO80* decreased after light treatment (*SI Appendix*, Fig. S3*F*). EYFP-AtINO80 protein levels displayed a similar trend as AtINO80-Flag, as determined by immunoblot analysis with an anti-GFP antibody, but to a lesser degree, i.e., mild increase during the transition from dark to light (Fig. 2*G* and *SI Appendix*, Fig. S3*G*) and decrease during the transition from light to dark (Fig. 2*H* and *SI Appendix*, Fig. S3*H*). We also detected more EYFP-AtINO80 protein in seedlings grown under strong white light than in weak white light or in the dark (Fig. 2*I* and *SI Appendix*, Fig. S3*I*).

Taken together, our results indicate that light can repress *AtINO80* mRNA levels but increase AtINO80 protein levels.

Effects of AtINO80 on the Transcriptome under Light and Dark Conditions. To identify AtINO80-regulated genes, we performed transcriptome deep sequencing (RNA-seq) to search for differentially expressed genes (DEGs) by comparing transcript levels between Col-0 and *atino80* seedlings. DESeq2 (28) was used to normalize the raw read counts from replicates, and the average value for each genotype was used to identify DEGs following the criteria: expression level change between mutant and wild type $|\log_2\text{foldchange}| \geq \log_2(1.5)$ and P value ≤ 0.05. To assess the effects due to light conditions, we analyzed DEGs by using plants grown under light and dark conditions.

First, we identified 3,735 DEGs in *atino80-5* plants grown under long-day conditions relative to Col-0 (Dataset S1). To look for genes responsible for the enhanced photomorphogenesis of *atino80* mutants, we compared these DEGs to 5,080 light-induced genes identified when seedlings were transferred from darkness to light conditions (29). We observed a substantial overlap ($P < 0.001$), with 29% of AtINO80-regulated genes among light-induced genes (Fig. 3*A* and Dataset S2). We then identified up (561)- and down

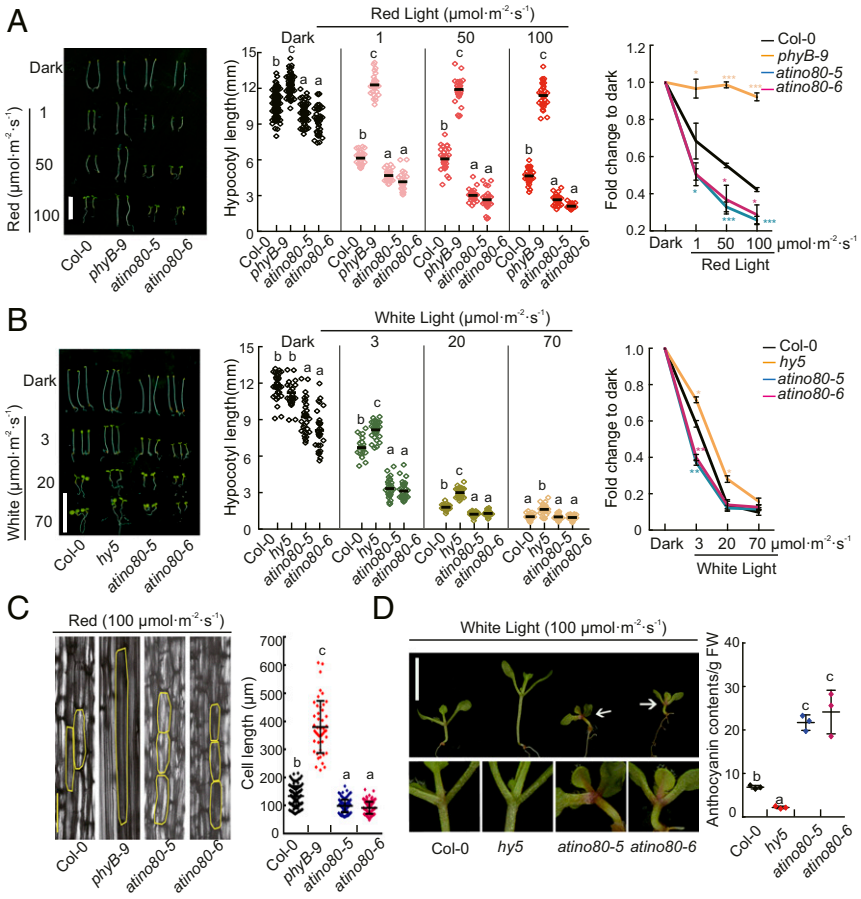

Fig. 1. Sensitivity of *atino80* mutants to light conditions. (*A* and *B*) Phenotypes of Col-0 (wild type) and *atino80* mutants under red (*A*) and white (*B*) light conditions. The *Left* panels represent images of 4-d-old seedlings grown in the dark and under a series of red (*A*) or white (*B*) light intensities. (Scale bar, 10 mm.) The *Middle* panels display the corresponding hypocotyl lengths ($n > 20$). Genotypes with different letters show significant differences ($P < 0.05$), as determined by Student's *t* test. The *Right* panels represent the fluence response curves of 4-d-old seedlings. Fold changes are calculated by comparing hypocotyl lengths under different light conditions to those in the dark. The data represent three independent biological replicates. Error bars represent SD. Asterisks indicate statistically significant differences between Col-0 and mutant seedlings according to Student's *t* test (*$P < 0.05$, **$P < 0.01$, ***$P < 0.001$). (*C*) Epidermal cell lengths of Col-0, *phyB-9*, and *atino80* seedlings in constant red light. Genotypes with different letters show significant differences ($P < 0.05$), as determined by Student's *t* test. (Scale bar, 100 μm.) (*D*) Anthocyanin contents of 7-d-old white light-grown seedlings. Genotypes with different letters show significant differences ($P < 0.05$), as determined by Student's *t* test. (Scale bar, 10 mm.)

(504)-regulated genes as those with expression changes above a $\log_2$(fold change) of 1.5 in either direction (shown as a dashed line) (Fig. 3*B*). We further performed Gene Ontology (GO) analysis of the genes belonging to each group. Representative categories based on biological function included "response to red light," "response to far-red light," and "response to light intensity" (Fig. 3*C* and Dataset S3). The enrichment of light-related GO terms was more significant among AtINO80 up-regulated groups than in the AtINO80 down-regulated groups. These results suggest that light-induced genes, specifically genes up-regulated by AtINO80, likely contribute to the enhanced photomorphogenesis of *atino80* plants.

Similarly, we identified 5,039 DEGs relative to Col-0 in dark-grown *atino80-6* seedlings (Dataset S4). To study the function of AtINO80 in skotomorphogenesis, we compared these DEGs with 4,468 dark-induced genes that were repressed in seedlings transferred from dark to light conditions (29). Approximately 23% of AtINO80-regulated genes were identified among dark-induced genes ($P < 0.001$) (Fig. 3*D* and Dataset S5). Of these, the expression levels of 379 genes increased while 780 genes decreased in abundance in *atino80-6* (Fig. 3*E*). GO analysis showed that the group of genes down-regulated by AtINO80 in the dark was most closely related to the "response to auxin," "cell maturation," and "cell wall thickening" categories (Fig. 3*F* and Dataset S6). These genes, related to cell elongation, may therefore contribute to the reduced skotomorphogenesis observed for *atino80*.

Expression of Light-Related Genes in *atino80* Mutants. To further explore the molecular mechanism by which AtINO80 regulates the photomorphogenesis/skotomorphogenesis switch, we wished to identify its putative target genes. Given the stronger phenotype of *atino80* mutant seedlings grown in white light, we validated the expression of several genes under these conditions. As shown in Fig. 3*G*, the transcript levels of *HY5*, *HYH*, *PAR1*, *SPATULA* (*SPT*), *NITRATE REDUCTASE* (*NIA2*), *MYC2*, *INDOLE-3-ACETIC ACID 7* (*IAA7*), *ETHYLENE RESPONSIVE ELEMENT BINDING FACTOR4* (*ERF4*), *ERF11*, and *APS REDUCTASE1* (*APR1*) greatly increased in the *atino80-5* and *atino80-6* mutant backgrounds grown in white light compared to Col-0, suggesting that AtINO80 indeed contributes to the repression of these genes (Fig. 3*G*). The increased transcript levels of anthocyanin biosynthesis genes (*CHALCONE SYNTHASE* [*CHS*] and *FLAVONOL SYNTHASE1* [*FLS1*]) was consistent with the accumulation of anthocyanins in *atino80* seedlings (Fig. 1*D*). We further examined whether AtINO80 regulates the expression levels of light signaling components such as phytochromes and PIFs. While the expression of *PHYB*, *CRY1*,

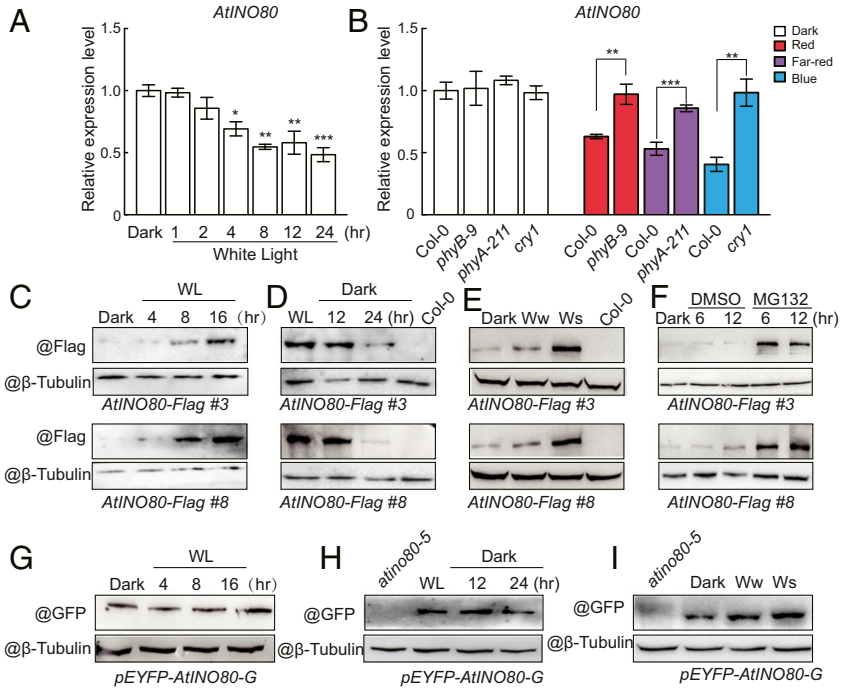

Fig. 2. Regulation of *AtINO80* by light. (*A*) *AtINO80* transcript levels in wild-type seedlings. Seedlings grown for 5 d in the dark were transferred to white light for 1 h, 2 h, 4 h, 8 h, 12 h, or 24 h. (*B*) RT-qPCR assays showing *AtINO80* expression in *phyB-9*, *phyA-211*, and *cry1* photoreceptor mutants grown in red, far-red, or blue light conditions, respectively. Data are shown as the mean and SD of three biological replicates normalized to reference *PP2A* in *A* and *B*. Asterisks indicate statistically significant differences between mean values according to Student's *t* test (*$P < 0.05$, **$P < 0.01$, ***$P < 0.001$). (*C–E*) AtINO80-Flag protein levels in *35S::AtINO80-Flag* transgenic seedlings exposed to different light conditions. *35S::AtINO80-Flag#3* (*Top*) and *35S::AtINO80-Flag#8* (*Bottom*) seedlings were grown in the dark and then treated with white light (WL, 120 $\mu mol \cdot m^{-2} \cdot s^{-1}$) (*C*), or seedlings were grown in white light for 7 d and then transferred to the dark (*D*), or seedlings were grown in constant darkness/weak white light (Ww, 4 $\mu mol \cdot m^{-2} \cdot s^{-1}$)/strong white light (Ws, 120 $\mu mol \cdot m^{-2} \cdot s^{-1}$) for 5 d (*E*). (*F*) AtINO80-Flag protein levels in *35S::AtINO80-Flag* transgenic seedlings grown in the dark and treated with DMSO (dimethyl sulfoxide) or 50 μM MG132 for 6 h and 12 h. (*G* and *H*) EYFP-AtINO80 protein levels in *pEYFP-AtINO80-G* transgenic seedlings exposed to different light conditions. *pEYFP-AtINO80-G* seedlings were grown in the dark and then exposed to white light (~120 $\mu mol \cdot m^{-2} \cdot s^{-1}$) (*G*), or seedlings were grown in white light for 7 d and then transferred to the dark (*H*), or seedlings were grown in the dark/weak white light (Ww, 4 $\mu mol \cdot m^{-2} \cdot s^{-1}$)/strong white light (Ws, 120 $\mu mol \cdot m^{-2} \cdot s^{-1}$) for 5 d (*I*). Immunoblotting against the anti-β-tubulin antibody served as a loading control.

PIF1, *PIF4*, and *PIF5* barely changed, the expression of *PIF7* significantly decreased in the *atino80-5* and *atino80-6* mutants (*SI Appendix*, Fig. S4*A*). The expression pattern of most tested genes displayed similar trends as the RNA-seq dataset (*SI Appendix*, Fig. S4 *B* and *C*). Interestingly, *HY5* transcript levels were reduced in the *atino80* mutants compared to Col-0 in the dark (*SI Appendix*, Fig. S4 *D* and *E*).

Changes of H3 Levels and H2A.Z Occupancy in *atino80*. As an ATP-dependent chromatin remodeler, yeast (*Saccharomyces cerevisiae*) INO80 causes the mobilization of nucleosomes and the preferential exchange of histone H2A.Z-H2B dimers out of nucleosomes (30). In *Arabidopsis*, a global defect of the histone H2A.Z landscape was not observed in the *atino80-1* mutant using 3-d-old etiolated seedlings (GSE122314) (31). To determine how AtINO80 regulates transcript levels, we performed chromatin immunoprecipitation followed by deep sequencing (ChIP-seq) using anti-histone H2A.Z and anti-histone H3 antibodies in long-day-grown Col-0 and *atino80-5* (*SI Appendix*, Fig. S5 *A* and *B*).

We obtained ~18,649 peaks (19,488 genes) for histone H2A.Z in Col-0 that largely overlapped (79%) with published histone H2A.Z ChIP-seq datasets (31) (*SI Appendix*, Fig. S5*C*). As shown in Fig. 4 *A* and *B*, histone H2A.Z was distributed across the gene body with a peak close to the transcription start site (TSS), consistent with previously published datasets (32, 33). In the *atino80-5* mutant, histone H2A.Z levels decreased across the entire gene body region (Fig. 4 *A* and *B*). Moreover, histone H3 occupancy was also altered in *atino80-5* (Fig. 4 *A* and *B*). Based on the input used as control, we identified 7,803 and 2,147 differentially enriched genes for histones H2A.Z and H3, respectively. The DEGs identified earlier in long-day-grown *atino80-5* significantly overlapped with the differentially histone H2A.Z- and H3-enriched genes (Fig. 4 *C* and *D*), indicating that the function of *AtINO80* is closely related to the level of histones H2A.Z and H3. Light-related GO terms were enriched in the two sets of overlapping genes (*SI Appendix*, Fig. S6 *A* and *B*). In addition, light-induced genes significantly overlapped with differentially histone H2A.Z- and histone H3-enriched genes (*SI Appendix*, Fig. S6 *C* and *D*).

Histone H2A.Z marks may be influenced by changes in histone H3 occupancy, because there is substantial overlap between differentially histone H3-enriched genes and differentially histone H2A.Z-enriched genes ($P < 0.001$) (Fig. 4*E* and Dataset S7). To this end, we determined significantly differential regions of histone H2A.Z enrichment relative to histone H3 occupancy by using histone H3 enrichment as input to perform differentially enrichment analysis of histone H2A.Z in all histone H2A.Z-enriched regions. In *atino80-5*, we identified 2,300 regions with reduced histone H2A.Z and 2,042 with increased histone H2A.Z (Fig. 4*F*). Up-regulated DEGs in *atino80-5* were significantly overrepresented in genes with reduced histone H2A.Z and down-regulated DEGs with increased histone H2A.Z (Fig. 4 *G* and *H*), suggesting a negative relationship between histone H2A.Z occupancy and transcription of AtINO80-regulated genes, which is consistent with recent reports (33–35).

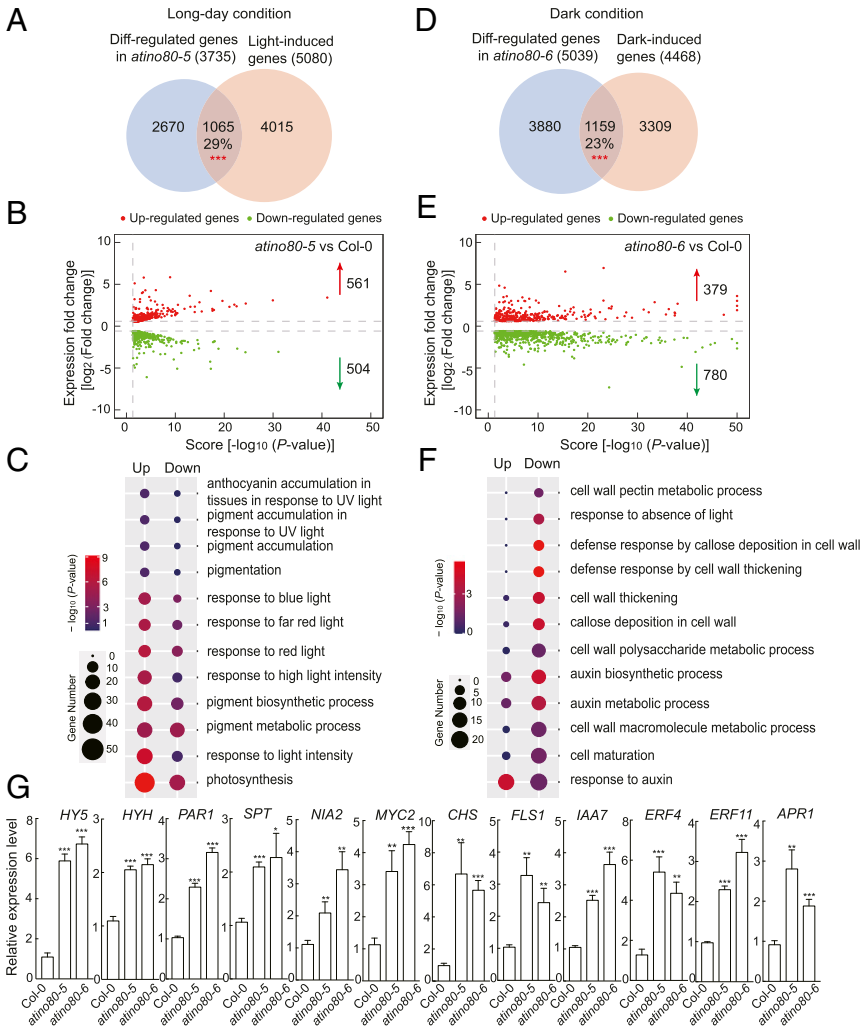

Fig. 3. AtINO80 regulates the expression of light-related genes. (*A*) Venn diagram comparing light-induced genes and differentially expressed genes in *atino80-5*. Two replicates were prepared for each genotype of plants grown under light. The significance level of the intersection was calculated by using Fisher's exact test (***$P < 0.001$). (*B*) Volcano plot representing the overlapping genes in *A*. The *y* axis indicates gene expression changes, and the *x* axis represents the significance scores in the *atino80-5* mutant compared with Col-0 seedlings. Red and green points represent up- and down-regulated genes, respectively. (*C*) GO analysis of up- and down-regulated genes shown in *B*. For each point, the size is proportional to the number of genes, and the colors represent the *P* value. (*D*) Venn diagram comparing dark-induced genes and differentially expressed genes in *atino80-6*. Three replicates were prepared for each genotype of plants grown under darkness. The significance level of the intersection was calculated with Fisher's exact test (***$P < 0.001$). (*E*) Volcano plot representing the overlapping genes in *D*. Red and green points represent up- and down-regulated genes, respectively. (*F*) GO analysis of up- and down-regulated genes shown in *E*. (*G*) Relative expression levels of *HY5*, *HYH*, *PAR1*, *SPT*, *NIA2*, *MYC2*, *CHS*, *FLS1*, *IAA7*, *ERF4*, *ERF11*, and *APR1* in Col-0 and *atino80* mutant seedlings grown in white light conditions. Seedlings were grown for 5 d in constant white light. Data are shown as the mean and SD of three biological replicates normalized to reference *PP2A*. Asterisks indicate statistically significant differences between mean values according to Student's *t* test (*$P < 0.05$, **$P < 0.01$, ***$P < 0.001$).

Mechanisms of the Regulation of Light-Related Genes by AtINO80. Next, we focused on light-responsive genes to determine the extent of changes in histone H2A.Z, H3, and the ratio of H2A.Z/H3 in transcription regulation by both light and AtINO80. We observed a reduction in histones H2A.Z/H3 in overlapping genes ($P < 0.05$, Fig. 5*A*), which was more pronounced for up-regulated genes in *atino80-5* relative to Col-0 ($P < 0.001$, Fig. 5*B*). However, the reduction in histones H2A.Z/H3 deposition was not significant among the down-regulated genes belonging to the cluster of overlapping light- and AtINO80-regulated genes ($P = 0.81$, Fig. 5*C*).

We tracked the levels of histones H2A.Z and H3 in selected genes. A decreased enrichment of histones H2A.Z and H3 across the gene bodies of *HY5*, *HYH*, *SPT*, *NIA2*, *FLS1*, and *EFR11* may result in their higher transcript levels in *atino80* (Figs. 5*D* and 3*G*). Notably, AtINO80 increased histones H2A.Z, H3, and H2A.Z/H3 enrichment at the *HY5* gene body and thus repressed the expression of *HY5*. HY5 is a key regulator in seedling photomorphogenesis that regulates the transcription of a wide range of genes. Therefore, the effect of AtINO80 on the expression of the genes listed above may be a consequence of changing histone H2A.Z levels and nucleosome density toward the transcriptional control of *HY5*.

A recent publication demonstrated that the primary activity of HY5 is in promoting transcription by directly targeting 127 genes (36). The DEGs identified in long-day-grown *atino80-5* significantly overlapped with these direct HY5-targeted genes ($P < 0.001$, Dataset S8). The function of AtINO80 on the expression of these overlapping HY5-targeted genes might be due to the reduction in histones H2A.Z and H3 levels, such as *RGA-LIKE3* (*RGL3*), microRNA 163 (miR163), *RESPONSIVE TO DESICCATION26*

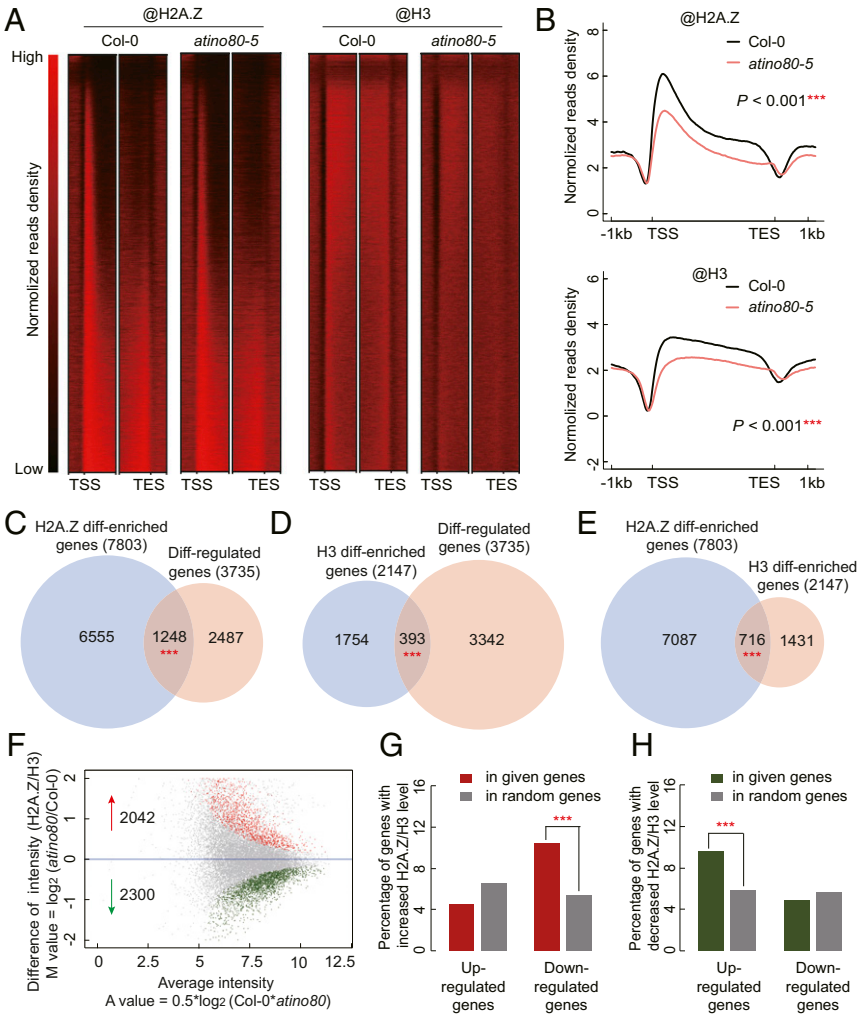

Fig. 4. Changes of histone H3 levels and histone H2A.Z occupancy in *atino80*. (*A*) Heatmap representation of genome-wide H2A.Z and H3 enrichment levels, from 1 kbp upstream of the transcription start site (TSS) to 1 kbp downstream of the transcription end site (TES) in Col-0 and the *atino80-5* mutant. Each row represents the normalized histone H2A.Z and H3 level over a gene. The gradient colors present the enrichment level. (*B*) Average density plot representing the distribution profile of histones H2A.Z and H3 in Col-0 and *atino80-5* mutant for all genes. The *P* value was calculated by Welch's *t* test (***$P < 0.001$). (*C* and *D*) Venn diagram of the overlap between DEGs and differentially H2A.Z- or H3-enriched genes (H2A.Z or H3 diff-enriched genes) in *atino80-5*. Significance level of the intersection was calculated by Fisher's exact test (***$P < 0.001$). (*E*) Venn diagram of the overlap between H2A.Z and H3 diff-enriched genes in *atino80-5*. Significance level of the intersection was calculated by Fisher's exact test (***$P < 0.001$). (*F*) MA plot for all histone H2A.Z-enriched regions (peaks) from comparison of *atino80* and Col-0 after normalization. Each dot represents a peak. The *x* axis is the A value, which presents the average intensity. The *y* axis is the M value, which presents the difference of the intensity (H2A.Z/H3). (*G* and *H*) Enrichment analysis of genes with increased or decreased histone H2A.Z/H3 levels among up- and down-regulated genes in *atino80-5*. Significance level was calculated using Fisher's exact test (***$P < 0.001$).

(*RD26*), At1g25400, and *CYS*, *MET*, *PRO*, *AND GLY PROTEIN1* (*CMPG1*) (*SI Appendix*, Fig. S7 *A* and *B*), and may also be a consequence of increased HY5 levels, such as for the At4g32480, *BTB AND TAZ DOMAIN PROTEIN 5* (*BT5*), *MYB44*, At4g38825, and *REDUCED EPIDERMAL FLUORESCENCE5* (*REF5*) genes (*SI Appendix*, Fig. S7 *C* and *D*).

AtINO80 regulated the transcription of several light-related genes, such as *EMPFINDLICHER IM DUNKELROTEN LICHT1* (*EID1*), *PHYTOCHROME KINASE SUBSTRATE4* (*PKS4*), *LOW-MOLECULAR-WEIGHT CYSTEINE-RICH68* (*LCR68*), *PLANTACYANIN* (*ARPN*), and *CASEIN ALPHA S1* (*CASA1*), solely by altering histone H2A.Z levels and not via HY5 (*SI Appendix*, Fig. S7 *E* and *F*).

In conclusion, the function of AtINO80 in light-regulated gene expression appears to be directly modulated by changing the nucleosome density and histone H2A.Z levels as well as indirectly mediated by its downstream genes, such as *HY5*.

***AtINO80* Acts in a *phyB*- and *HY5*-Dependent Manner.** To assess AtINO80 function in relation to the master light signaling component HY5, we first validated the histone H2A.Z and H3 levels on the *HY5* gene body in the *atino80* mutant through ChIP-qPCR. As shown in Fig. 6*A*, histones H2A.Z and H3 were mainly enriched and distributed in the *HY5* gene body close to the TSS (P3 fragment) in Col-0 and significantly decreased in the *atino80* mutant. We then analyzed the binding of AtINO80 across the *HY5* gene body by using a *35S::AtINO80-Flag* transgenic line. AtINO80 bound the *HY5* gene body where histone H2A.Z localized (Fig. 6*B*), indicating a direct role for AtINO80 in *HY5* transcriptional regulation. Previous reports have shown that the DBINO domain of human and *Drosophila* INO80/Ino80 proteins interacts with DNA holding a specific DNA sequence motif 5′[CA][CA][CA][CG]GTCA[GC]CC3′ (37, 38). Close to the region of the P3 fragment, the sequence 5′ACCGGTCAG3′ on the *HY5* gene body might mediate the binding of AtINO80.

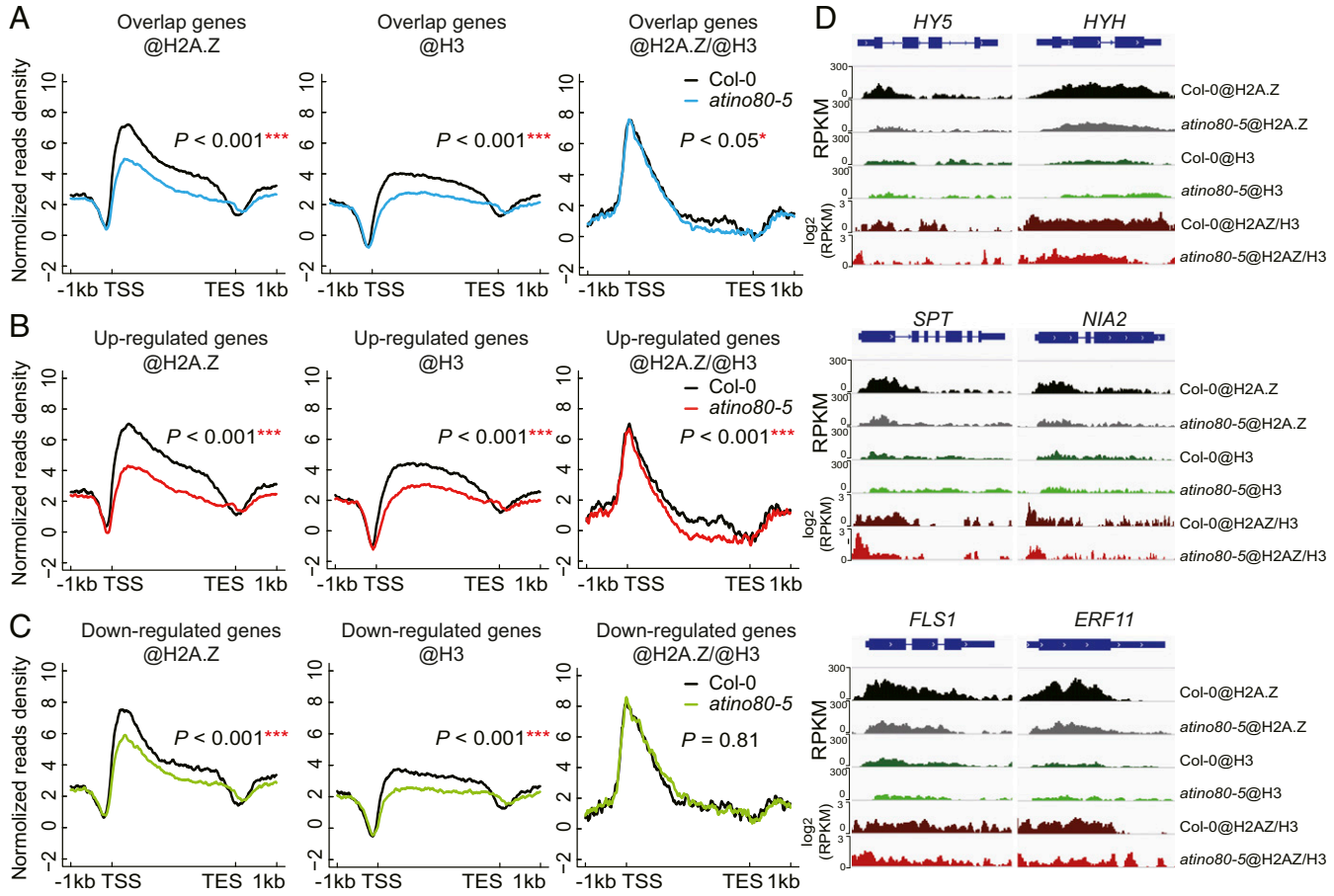

Fig. 5. Histone H2A.Z and H3 occupancy changes in overlapping AtINO80-regulated and light-induced genes. (*A*–*C*) Average density plot representing the distribution profile of histones H2A.Z, H3, and H2A.Z/H3 in Col-0 and *atino80-5* mutant in all, up- and down-regulated genes of overlapping genes. The *P* value was calculated by Welch's *t* test (***$P < 0.001$). (*D*) Integrative Genomics Viewer (IGV) screen shots showing the distribution of H2A.Z, H3 and H2A.Z/H3 enrichment level in Col-0 and *atino80-5* mutant at the *HY5*, *HYH*, *SPT*, *NIA2*, *FLS1*, and *ERF11* loci. RPKM: reads per kilobase per million mapped reads.

Next, we detected the levels of HY5 protein in Col-0 and *atino80* mutants (Fig. 6*C*). Quantitative immunoblot analyses indicated that HY5 protein is about 1.7 times more abundant in *atino80* than in Col-0 under white light conditions. However, etiolated Col-0 and *atino80* seedlings showed the same drastically low levels of HY5 (Fig. 6*C*).

To determine the nature of the genetic interaction between *AtINO80* and light signaling components (*phyB*/*HY5*/*COP1*), we generated double mutants and examined their hypocotyl phenotype. The *atino80-6 phyB-9* double mutant exhibited an obviously shorter hypocotyl than *phyB-9* (Fig. 6 *D* and *E* and *SI Appendix*, Fig. S8), with a decrease of 46%, from 11.3 mm (*phyB-9*) to 6.0 mm (*atino80-6 phyB-9*), in red light, and of 45%, from 4.0 mm (*phyB-9*) to 2.2 mm (*atino80-6 phyB-9*), in white light, suggesting that *AtINO80* probably acts downstream of phytochromes. Next we tested the epistasis between *atino80* and *hy5* (Fig. 6 *E* and *F* and *SI Appendix*, Fig. S8): in this mutant combination, hypocotyl length only decreased by 13.8% (in white light), 19.6% (in red), 29.6% (in blue), and 19.7% (in far-red) in *atino80-6 hy5* compared to *hy5*, suggesting that the function of *AtINO80* is largely dependent on *HY5*. Lastly, we examined the relationship between *atino80-6* and the weak allele *cop1-4*. In contrast to the hypocotyl length of *atino80-5*, the *atino80-5 cop1-4* double mutant exhibited a much shorter hypocotyl in both white light and dark conditions (Fig. 6*G*), revealing that *atino80* exhibits a *cop*-like mutant hypocotyl phenotype.

Discussion

INO80 causes growth arrest and embryo death in *Drosophila* and mice, which leads to difficulties in understanding the molecular mechanism as well as the biological function of this protein. By contrast, *atino80* mutants are viable and thus offer the unique opportunity to study the genome-wide effects of a loss of AtINO80 function during development. Loss of *AtINO80* was first reported to affect DNA damage repair and homologous chromosome recombination (39, 40). Further studies indicated that *AtINO80* plays an important role in controlling flowering time (24, 41). Together with *APR5*, *AtINO80* was recently shown to play a role in plant cellular proliferation and replication stress responses (41). Here, we reveal a function for *AtINO80* in photomorphogenesis and skotomorphogenesis in *Arabidopsis*.

Light can influence the expression levels of several chromatin remodeling factors. For example, the transcription of *PKL* is repressed by light (17), whereas the protein levels of BAF60 can be stabilized by light (18). The effects of light on the transcriptional and translational regulation of *AtINO80*/AtINO80 take on opposite directions (Fig. 2). These opposite regulatory patterns have been observed for some light signaling components, such as PIF4/5 (42) and BBX21 (43).

Our global gene expression study demonstrated that AtINO80 plays a critical role in light-regulated gene expression under both light and dark conditions (Figs. 2 and 3). However, the effect of AtINO80 on skotomorphogenesis is minimal. Although a dataset related to nucleosome composition in etiolated *atino80* seedlings

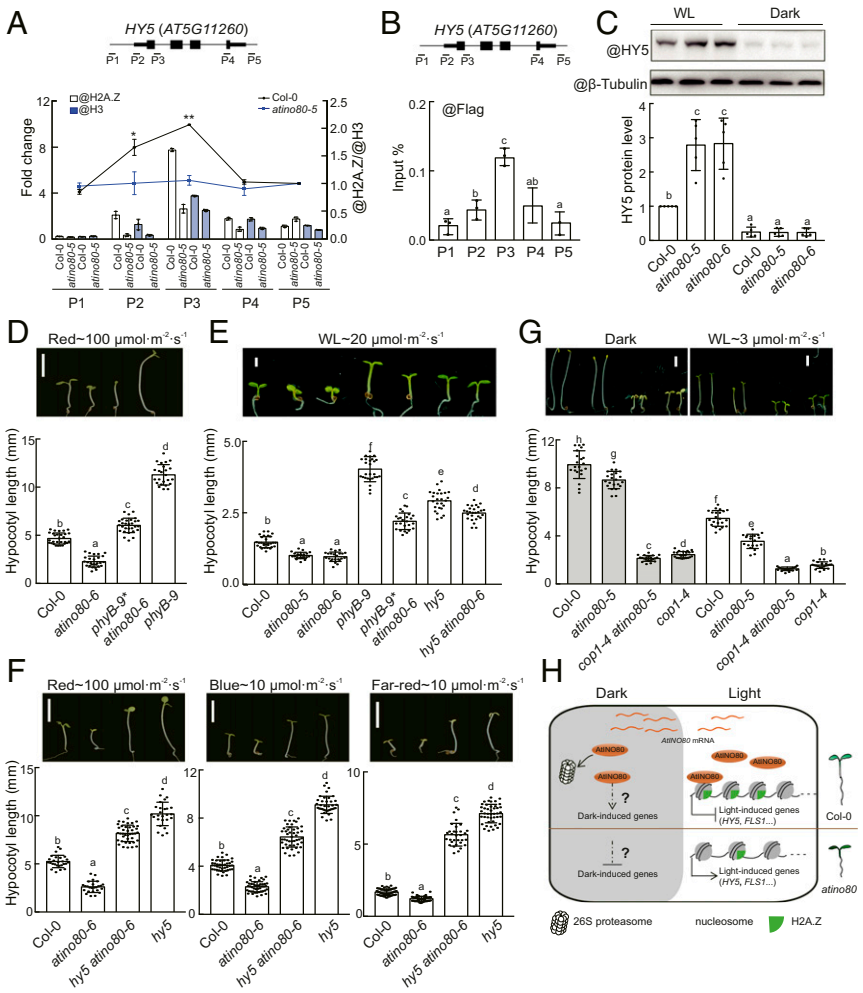

Fig. 6. AtINO80 regulates photomorphogenesis in a phyB- and HY5-dependent manner. (*A*) ChIP-PCR analysis using anti-H2A.Z and anti-H3 antibodies in various regions of *HY5* chromatin in Col-0 and *atino80-5* seedlings. The *Top* shows a schematic representation of the *HY5* gene structure. The bars labeled with numbers represent regions examined by PCR. A region of *PP2A* served as an internal control and was used in normalization. The *Right y* axis represents the mean ratio of H2A.Z to H3 in Col-0 and *atino80-5*. (*B*) ChIP-PCR analysis using anti-Flag agarose in various regions of *HY5* chromatin in *35S::AtINO80-Flag* seedlings. (*C*) HY5 protein levels in Col-0 and *atino80* mutants under light and dark conditions. The *Upper* panel represents HY5 protein levels in Col-0 and *atino80* mutants seedlings grown in constant light or darkness for 5 d. The *Bottom* represents quantified HY5 protein levels from the *Upper* panels. Protein levels were normalized to that of the loading control at each time point. Data are shown as the mean and SD of five biological replicates. Bars with different letters show significant differences ($P < 0.05$) as determined by Student's *t* test. (*D*) Phenotypes of Col-0, *atino80-6*, *phyB-9*, and *phyB-9 atino80-6* seedlings grown under red light. Seedlings were grown in constant red light for 5 d. (*E*) Phenotypes of seedlings in constant white light conditions. Seedlings were grown in white light for 4 d. (*F*) Phenotypes of Col-0, *atino80-6*, *hy5*, and *hy5 atino80-6* seedlings in red, blue, and far-red light conditions. Seedlings were grown for 5 d. (*G*) Phenotypes of seedlings in the dark or in weak white light conditions. Seedlings were grown in the dark or in weak white light for 5 d. Bars with different letters show significant differences ($P < 0.05$) as determined by Student's *t* test. (*H*) Model illustrating the role of AtINO80. In the dark, AtINO80 protein levels are subjected to degradation by the 26S proteasome, and mutation of AtINO80 leads to reduced expression of dark-induced genes but the underlying mechanism remains unknown. In the light, AtINO80 attenuates the transcription of light-induced genes (e.g., *HY5* and *FLS1*) via nucleosome occupancy and H2A.Z enrichment, playing an essential function in plant photomorphogenesis.

is currently not available, the global histone H2A.Z landscape was not affected in *atino80-1* compared to wild-type when 3-d-old etiolated seedlings were analyzed (GSE122314) (31). In our study, we determined that AtINO80 affects the nucleosome density and histone H2A.Z enrichment in the *HY5* gene body and other light-related genes under light conditions (Fig. 5), thereby repressing their expression (Fig. 3). A genetic analysis indicated that the function of AtINO80 is dependent on HY5 (Fig. 6). Although the expression of *PIF7* decreased in *atino80* (*SI Appendix*, Fig. S4*A*), histone H2A.Z and H3 levels at the *PIF7* locus do not change (*SI Appendix*, Fig. S9). AtINO80 might therefore not directly regulate the transcription of *PIF7*.

How the INO80 complex modulates histone H2A.Z levels in chromatin remains to be addressed (44). Previous studies have shown that in yeast cells, the INO80 complex is able to replace histone H2A.Z/H2B dimers with a canonical H2A/H2B dimer and modulate the acetylation of histone H2A.Z (25). In human cells, the INO80 complex removes histone H2A.Z from chromatin on both sides of a DNA damage site and promotes homologous recombination (45). However, a study in yeast also showed that the deletion of INO80 did not affect histone H2A.Z occupancy (46). In our study, ChIP-seq data revealed that histone H3 occupancy and the enrichment of histone H2A.Z in gene body regions significantly decreased in the *atino80* mutant (Fig. 4). The altered histone H3 density might be the reason for the exchange of histone H2A.Z with H2A (30). How the INO80 complex affects histone H3 density and thereby changes the distribution of histone H2A.Z in the genome will require further work.

Histone H2A.Z is a conserved variant of histone H2A and has been reported to be involved in many biological processes, including DNA repair, heterochromatin establishment, transcriptional regulation, and responses to the environment (21, 35, 39). Histone H2A.Z exhibits a conserved distribution around TSS but is also enriched across the body of genes related to stimulus response (34). To evaluate the role of histone H2A.Z independently from histone H3 changes, we defined significantly different regions of histone H2A.Z enrichment relative to histone H3 occupancy by employing DESeq-like analysis (Fig. 4*F*). Our data demonstrated that changes in histone H2A.Z enrichment at gene bodies is negatively correlated with gene expression changes (Fig. 4 *G* and *H*), which reinforced the conclusion of the negative regulatory role of histone H2A.Z on transcription (33–35). Focusing on the overlapping genes between AtINO80-regulated and light-induced genes, the negative regulation of histones H2A.Z/H3 on transcription appears in up-regulated genes, but not in down-regulated genes (Fig. 5 *B* and *C*), which suggests that down-regulation of these genes may be regulated indirectly or through another yet unknown mechanism by AtINO80. It has been reported that histone H2A.Z is partially associated with H3K27me3 deposition (22, 34). A lack of AtINO80 results in a global decrease in histone H2A.Z levels in the gene body (Fig. 4*B*), probably resulting in a change in H3K27me3 levels. Recent research suggested that the repressive role of histone H2A.Z in gene expression depends on monoubiquitination by the Polycomb Repressive Complex 1 (PRC1) components BMI1A/B/C (35). AtINO80 may work together with PRC1 to promote gene repression, which will be a future research direction.

Based on our results, we propose a working model for the chromatin remodeler AtINO80 during photomorphogenesis (Fig. 6*H*). In the dark, *AtINO80* mRNA accumulates while the AtINO80 protein is degraded by the 26S proteasome. AtINO80 affects the expression of dark-induced genes with an unknown mechanism. In the light, AtINO80 protein levels increase and affect the nucleosome density (histone H3 level) as well as the occupancy of histone H2A.Z on light-related genes, thereby modulating their expression. Chromatin-based transcriptional regulation may thus greatly improve robustness and adaptivity to environmental changes in plants.

Methods

Detailed descriptions of measurements of hypocotyl length, cell length, and anthocyanin contents; quantitative RT-PCR analysis; RNA-seq and ChIP-seq library preparation, construction, and analysis; antibody information; and accession numbers are provided in *SI Appendix, Methods*.

Plant Materials and Growth Conditions. All *A. thaliana* genotypes used in this study were of the Columbia accession. The *atino80-5* (SALK_036887) and *atino80-6* (GK_223B11) mutants, and the *pEYFP-AtINO80-G/atino80-5* transgenic line were described previously (24). *hy5* mutant allele information is provided in refs. 36, 47. The *cop1-4*, *phyA-211*, and *phyB-9* mutants were also described previously (5). Double mutants were generated by genetic crossing and verified by phenotypic inspection, PCR genotyping, and/or sequencing. The full-length cDNA of *AtINO80* was amplified by PCR and ligated into the *Kpn*I and *Sal*I sites of pCAMBIA1306 to generate pCAMBIA1306-AtINO80-3xFlag. This construct was introduced into *Agrobacterium* (*Agrobacterium tumefaciens*) strain GV3101 and used for plant transformation. Transgenic lines overexpressing AtINO80-Flag were screened on half-strength Murashige and Skoog (1/2 MS) nutrient medium containing 50 mg/mL hygromycin and confirmed by immunoblot analysis with antibodies against Flag (GNI, GNI4110-FG).

RNA-Seq Library Preparation, Construction, and Analysis. See *SI Appendix, Methods* for a detailed description of analytical methods. In brief, wild-type and *atino80* plants were grown under long-day conditions for 14 d or grown for 4 d in constant darkness. Two replicates and three replicates were prepared for each genotype of plants grown under light and dark conditions, respectively. Total RNA was extracted from snap-frozen tissues using TRIzol reagent according to the manufacturer's instructions (Invitrogen). RNA libraries were constructed and sequenced by GENERGY (http://www.genenergy.cn/) and Majorbio (http://www.majorbio.com/). Differential expression analysis was performed using DESeq2 (28) with $|\log_2\text{foldchange}| \geq \log_2(1.5)$ and P value ≤ 0.05 (Datasets S1 and S4). Statistics of detailed RNA-seq reads are given in Dataset S9.

ChIP-Seq Library Preparation, Construction, and Analysis. See *SI Appendix, Methods* for a detailed description of analytical methods. ChIP assays were performed with antibodies against histones H2A.Z or H3 as previously described (24). The ChIP-seq libraries were constructed as previously described (48). The libraries were sequenced on an Illumina HiSeq2000 instrument as 50-bp paired-end reads. H2A.Z and H3 enrichment regions and differentially enriched peaks were identified by SICER (49) with the input library as control. In order to determine the specific differential enrichment regions of H2A.Z relative to H3 occupancy, we used DiffBind (50) to perform an enrichment analysis with the H3 library as control, which utilized the DESeq2 (28) method and considered occupancy differences in the control. Statistics of detailed ChIP-seq reads are given in Dataset S9.

Data Availability. The raw and processed data of RNA-seq and ChIP-seq generated in this study have been deposited at the National Center for Biotechnology Information GEO database with accession numbers GSE150116 and GSE149841, respectively.

ACKNOWLEDGMENTS. This research was supported by the National Natural Science Foundation of China (NSFC32030018,31930017) and the National Key R&D Program of China (2017YFA0503800); and W.-H.S. received support from the Centre National de la Recherche Scientifique (Laboratoire International Associé Plant Epigenetic Research) and the Agence National de la Recherche (ANR-19-CE20-0018).

1. A. Von Arnim, X. W. Deng, Light control of seedling development. *Annu. Rev. Plant Physiol. Plant Mol. Biol.* **47**, 215–243 (1996).
2. V. C. Galvão, C. Fankhauser, Sensing the light environment in plants: Photoreceptors and early signaling steps. *Curr. Opin. Neurobiol.* **34**, 46–53 (2015).
3. O. S. Lau, X. W. Deng, The photomorphogenic repressors COP1 and DET1: 20 years later. *Trends Plant Sci.* **17**, 584–593 (2012).
4. P. Zhou *et al*., Both PHYTOCHROME RAPIDLY REGULATED1 (PAR1) and PAR2 promote seedling photomorphogenesis in multiple light signaling pathways. *Plant Physiol.* **164**, 841–852 (2014).
5. L. H. Ang *et al*., Molecular interaction between COP1 and HY5 defines a regulatory switch for light control of Arabidopsis development. *Mol. Cell* **1**, 213–222 (1998).
6. T. Oyama, Y. Shimura, K. Okada, The Arabidopsis HY5 gene encodes a bZIP protein that regulates stimulus-induced development of root and hypocotyl. *Genes Dev.* **11**, 2983–2995 (1997).
7. M. T. Osterlund, C. S. Hardtke, N. Wei, X. W. Deng, Targeted destabilization of HY5 during light-regulated development of Arabidopsis. *Nature* **405**, 462–466 (2000).
8. J. Lee *et al*., Analysis of transcription factor HY5 genomic binding sites revealed its hierarchical role in light regulation of development. *Plant Cell* **19**, 731–749 (2007).
9. V. N. Pham, X. Xu, E. Huq, Molecular bases for the constitutive photomorphogenic phenotypes in *Arabidopsis*. *Development* **145**, dev169870 (2018).
10. J. J. Ling, J. Li, D. Zhu, X. W. Deng, Noncanonical role of *Arabidopsis* COP1/SPA complex in repressing BIN2-mediated PIF3 phosphorylation and degradation in darkness. *Proc. Natl. Acad. Sci. U.S.A.* **114**, 3539–3544 (2017).
11. P. Leivar, P. H. Quail, PIFs: Pivotal components in a cellular signaling hub. *Trends Plant Sci.* **16**, 19–28 (2011).
12. Y. L. Chua, L. A. Watson, J. C. Gray, The transcriptional enhancer of the pea plastocyanin gene associates with the nuclear matrix and regulates gene expression through histone acetylation. *Plant Cell* **15**, 1468–1479 (2003).
13. M. Benhamed, C. Bertrand, C. Servet, D. X. Zhou, Arabidopsis GCN5, HD1, and TAF1/HAF2 interact to regulate histone acetylation required for light-responsive gene expression. *Plant Cell* **18**, 2893–2903 (2006).
14. X. Liu *et al*., PHYTOCHROME INTERACTING FACTOR3 associates with the histone deacetylase HDA15 in repression of chlorophyll biosynthesis and photosynthesis in etiolated Arabidopsis seedlings. *Plant Cell* **25**, 1258–1273 (2013).
15. D. Gu *et al*., Identification of HDA15-PIF1 as a key repression module directing the transcriptional network of seed germination in the dark. *Nucleic Acids Res.* **45**, 7137–7150 (2017).
16. L. Zhao *et al*., HY5 interacts with the histone deacetylase HDA15 to repress hypocotyl cell elongation in photomorphogenesis. *Plant Physiol.* **180**, 1450–1466 (2019).
17. Y. Jing *et al*., Arabidopsis chromatin remodeling factor PICKLE interacts with transcription factor HY5 to regulate hypocotyl cell elongation. *Plant Cell* **25**, 242–256 (2013).
18. T. Jégu *et al*., The Arabidopsis SWI/SNF protein BAF60 mediates seedling growth control by modulating DNA accessibility. *Genome Biol.* **18**, 114 (2017).
19. M. Peng *et al*., Linking PHYTOCHROME-INTERACTING FACTOR to histone modification in plant shade avoidance. *Plant Physiol.* **176**, 1341–1351 (2018).

20. A. Nassrallah *et al*., DET1-mediated degradation of a SAGA-like deubiquitination module controls H2Bub homeostasis. *eLife* **7**, e37892 (2018).
21. S. V. Kumar, P. A. Wigge, H2A.Z-containing nucleosomes mediate the thermosensory response in Arabidopsis. *Cell* **140**, 136–147 (2010).
22. W. Sura *et al*., Dual role of the histone variant H2A.Z in transcriptional regulation of stress-response genes. *Plant Cell* **29**, 791–807 (2017).
23. R. Ebbert, A. Birkmann, H. J. Schüller, The product of the SNF2/SWI2 paralogue INO80 of Saccharomyces cerevisiae required for efficient expression of various yeast structural genes is part of a high-molecular-weight protein complex. *Mol. Microbiol.* **32**, 741–751 (1999).
24. C. Zhang *et al*., The chromatin-remodeling factor AtINO80 plays crucial roles in genome stability maintenance and in plant development. *Plant J.* **82**, 655–668 (2015).
25. M. Papamichos-Chronakis, S. Watanabe, O. J. Rando, C. L. Peterson, Global regulation of H2A.Z localization by the INO80 chromatin-remodeling enzyme is essential for genome integrity. *Cell* **144**, 200–213 (2011).
26. S. D. Neuman, R. J. Ihry, K. M. Gruetzmacher, A. Bashirullah, INO80-dependent regression of ecdysone-induced transcriptional responses regulates developmental timing in Drosophila. *Dev. Biol.* **387**, 229–239 (2014).
27. J. N. Min *et al*., The mINO80 chromatin remodeling complex is required for efficient telomere replication and maintenance of genome stability. *Cell Res.* **23**, 1396–1413 (2013).
28. M. I. Love, W. Huber, S. Anders, Moderated estimation of fold change and dispersion for RNA-seq data with DESeq2. *Genome Biol.* **15**, 550 (2014).
29. N. Sun *et al*., Arabidopsis SAURs are critical for differential light regulation of the development of various organs. *Proc. Natl. Acad. Sci. U.S.A.* **113**, 6071–6076 (2016).
30. S. Brahma *et al*., INO80 exchanges H2A.Z for H2A by translocating on DNA proximal to histone dimers. *Nat. Commun.* **8**, 15616 (2017).
31. M. Zander *et al*., Epigenetic silencing of a multifunctional plant stress regulator. *eLife* **8**, e47835 (2019).
32. E. S. Torres, R. B. Deal, The histone variant H2A.Z and chromatin remodeler BRAHMA act coordinately and antagonistically to regulate transcription and nucleosome dynamics in Arabidopsis. *Plant J.* **99**, 144–162 (2019).
33. X. Dai *et al*., H2A.Z represses gene expression by modulating promoter nucleosome structure and enhancer histone modifications in Arabidopsis. *Mol. Plant* **10**, 1274–1292 (2017).
34. D. Coleman-Derr, D. Zilberman, Deposition of histone variant H2A.Z within gene bodies regulates responsive genes. *PLoS Genet.* **8**, e1002988 (2012).
35. Á. Gómez-Zambrano, W. Merini, M. Calonje, The repressive role of Arabidopsis H2A.Z in transcriptional regulation depends on AtBMI1 activity. *Nat. Commun.* **10**, 2828 (2019).
36. Y. Burko *et al*., Chimeric activators and repressors define HY5 activity and reveal a light-regulated feedback mechanism. *Plant Cell* **32**, 967–983 (2020).
37. S. Mendiratta, S. Bhatia, S. Jain, T. Kaur, V. Brahmachari, Interaction of the chromatin remodeling protein hINO80 with DNA. *PLoS One* **11**, e0159370 (2016).
38. S. Jain, J. Maini, A. Narang, S. Maiti, V. Brahmachari, The regulatory function of dIno80 correlates with its DNA binding activity. *Gene* **732**, 144368 (2020).
39. W. Zhou *et al*., Distinct roles of the histone chaperones NAP1 and NRP and the chromatin-remodeling factor INO80 in somatic homologous recombination in Arabidopsis thaliana. *Plant J.* **88**, 397–410 (2016).
40. O. Fritsch, G. Benvenuto, C. Bowler, J. Molinier, B. Hohn, The INO80 protein controls homologous recombination in Arabidopsis thaliana. *Mol. Cell* **16**, 479–485 (2004).
41. H. Kang, C. Zhang, Z. An, W. H. Shen, Y. Zhu, AtINO80 and AtARP5 physically interact and play common as well as distinct roles in regulating plant growth and development. *New Phytol.* **223**, 336–353 (2019).
42. Y. Shen, R. Khanna, C. M. Carle, P. H. Quail, Phytochrome induces rapid PIF5 phosphorylation and degradation in response to red-light activation. *Plant Physiol.* **145**, 1043–1051 (2007).
43. D. Xu *et al*., BBX21, an Arabidopsis B-box protein, directly activates HY5 and is targeted by COP1 for 26S proteasome-mediated degradation. *Proc. Natl. Acad. Sci. U.S.A.* **113**, 7655–7660 (2016).
44. F. Wang, A. Ranjan, D. Wei, C. Wu, Comment on "A histone acetylation switch regulates H2A.Z deposition by the SWR-C remodeling enzyme". *Science* **353**, 358 (2016).
45. H. E. Alatwi, J. A. Downs, Removal of H2A.Z by INO80 promotes homologous recombination. *EMBO Rep.* **16**, 986–994 (2015).
46. C. Jeronimo, S. Watanabe, C. D. Kaplan, C. L. Peterson, F. Robert, The histone chaperones FACT and Spt6 restrict H2A.Z from intragenic locations. *Mol. Cell* **58**, 1113–1123 (2015).
47. X. Chen *et al*., Shoot-to-Root mobile transcription factor HY5 coordinates plant carbon and nitrogen acquisition. *Curr. Biol.* **26**, 640–646 (2016).
48. A. Barski *et al*., High-resolution profiling of histone methylations in the human genome. *Cell* **129**, 823–837 (2007).
49. C. Zang *et al*., A clustering approach for identification of enriched domains from histone modification ChIP-Seq data. *Bioinformatics* **25**, 1952–1958 (2009).
50. C. S. Ross-Innes *et al*., Differential oestrogen receptor binding is associated with clinical outcome in breast cancer. *Nature* **481**, 389–393 (2012).